Modeling and Optimization of an Electric Drive System with Dual-Zone Speed Regulation

Mikho R. Mikhov[1], Boyan G. Balev[2]

Abstract – **The performance of a DC electric drive system with dual-zone speed regulation has been discussed in this paper. Detailed investigation and analysis by means of modeling and computer simulation have been carried out for different loads at the respective transient and steady state regimes. The developed models and the results obtained can be used in optimization and final tuning of such types of speed control drive systems.**

Keywords – **Electric drive system, Dual-zone speed regulation.**

I. INTRODUCTION

By technological reasons dual-zone speed regulation is often required in industrial automation. Regulation is carried out at constant motor torque until a basic speed level is reached. After that, it is realized at constant power. The rated speed is most often regarded as basic speed value.

Usually one of the two fundamental principles of control are being employed in the electric drive systems with dual-zone speed regulation, namely:

a) independent control;

b) dependent control.

In the first case, up to a reference value of the input signal, the control is carried out through the armature voltage; above this value it is realized by the motor excitation current, at constant armature voltage.

By the second principle, for the entire range of speed regulation, control is done by the armature voltage, as the excitation current change is a function either of the back electromotive force (EMF) voltage, or of the armature voltage.

A distinctive feature of the dual-zone speed regulation is that the system structure changes along the process of regulation and the optimal coordination of zones creates the main control problem.

Mathematical modeling and computer simulation offer effective ways to investigate the electric drive systems in details, in various dynamic and static working regimes, especially when it is not possible or is inconvenient to carry out such tests in laboratory or industrial environments [4].

This paper discusses a DC electric drive system with dual-zone speed regulation, where control shift is a function of the motor back EMF voltage. Through modeling and computer simulation, operation in the transient and steady state regimes has been analyzed, at various loads and disturbances applied to the motor shaft. Some results from these investigations are reported.

[1]Mikho R. Mikhov is with the Faculty of Automatics, Technical University of Sofia, 8 Kliment Ohridski Str., 1797 Sofia, Bulgaria, E-mail: mikhov@tu-sofia.bg

[2]Boyan G. Balev is with Kontrax Ltd., 13 Tintiava Str., 1113 Sofia, Bulgaria, E-mail: bbalev@kontrax.bg

II. FEATURES OF THE ELECTRIC DRIVE SYSTEM

The electric drive system block diagram is shown in Fig. 1, where the following notations have been used: $G_{sc}(s)$ - transfer function of the speed controller; $G_{c_1 c}(s)$ - transfer function of the armature current controller; K_{p_1} and τ_{p_1} - gain and delay of the armature voltage power converter; $R_{1\Sigma}$ - armature circuit resistance; $\tau_{1\Sigma}$ - armature circuit time-constant; $K_{c_1 f}$ and $\tau_{c_1 f}$ - gain and time-constant of the armature current feedback; K_{sf} and τ_{sf} - gain and time-constant of the speed feedback; $G_{ec}(s)$ - transfer function of the back EMF voltage controller; $G_{c_2 c}(s)$ - transfer function of the excitation current controller; K_{p_2} and τ_{p_2} - gain and delay of the excitation voltage power converter; $R_{2\Sigma}$ - excitation circuit resistance; $\tau_{2\Sigma}$ - excitation circuit time-constant; $K_{c_2 f}$ and $\tau_{c_2 f}$ - gain and time-constant of the excitation current feedback; K_{ef} и τ_{ef} - gain and time-constant of the back EMF voltage feedback; K_{Φ} - coefficient of the magnetic flux curve gradient; c' и c'' - motor coefficients; V_{sr} - speed reference signal; V_{sf} - speed feedback signal; $V_{c_1 r}$ - armature current reference signal; $V_{c_1 f}$ - armature current feedback signal; V_1 - armature voltage; I_1 - armature current; T - motor torque; T_l - load torque applied to the motor shaft; J_{Σ} - total inertia referred to the motor shaft; ω - angular motor speed; V_{er} - back EMF voltage reference signal; V_{ef} - back EMF voltage feedback signal; $V_{c_2 r}$ - excitation current reference signal; $V_{c_2 f}$ - excitation current feedback signal; V_2 - excitation voltage; I_2 - excitation current; Φ - magnetic flux.

The electric drive system under consideration consists of two interrelated subsystems:

a) dual-loop subsystem for speed regulation, which includes an external speed loop and a subordinated armature current loop;

b) dual-loop subsystem for back EMF voltage regulation, including external back EMF voltage loop and subordinated excitation current loop.

Speed regulation until the value of $\omega \le \omega_{rat}$ is carried out at rated magnetic flux $(\Phi = \Phi_{rat})$, at the expense of the armature voltage change. At $\omega > \omega_{rat}$ the regulation is done
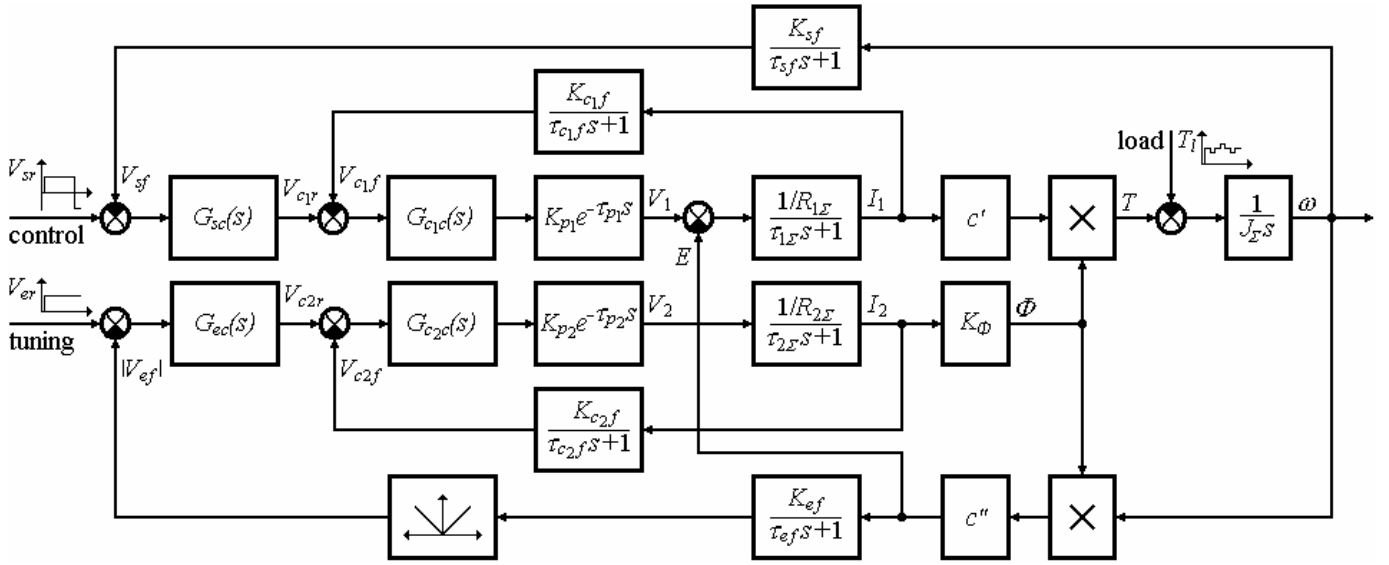
Fig. 1. Block diagram of the discussed electric drive

through the flux reduction $(\Phi < \Phi_{\mathrm{rat}})$.

Within the entire range, speed is set up by the control signal V_{sr}, while through the tuning signal V_{er} a back EMF voltage, determining the basic speed is defined.

If the electric drive system should be of four-quadrant type with both current and speed reversion, the power converter for armature voltage is of reversive type, while the power converter for the excitation voltage is non-reversive. If speed direction changes, the feedback signal sign of V_{ef} changes, but the V_{er} signal remains with the same sign. For that reason, to avoid the V_{ef} sign influence, in four-quadrant drive systems an absolute value block is included.

III. SYNTHESIS OF BACK EMF VOLTAGE SENSOR

In order to receive information about the back EMF voltage, a suitable sensor has been developed. The block diagram, illustratig the prosses of obtaining information about the back EMF voltage is shown in Fig. 2, where the used notations are as follows: $G_{vs}(s)$ - transfer function of the voltage sensor; $G_{cs}(s)$ - transfer function of the current sensor.

Evaluation of the back EMF voltage is carried out on the basis of a signal, proportional to the armature voltage and a signal about the armature current compensation, proportional to the voltage fall in R_a, i.e.:

$$V_{ef}(s) = V_v(s) - V_c(s). \qquad (1)$$

Depending on both the voltage sensor and current sensor transfer functions, diverse back EMF voltage transfer functions $G_{es}(s)$ can be obtained.

Several versions have been explored to select the most appropriate pair. The one with the following transfer functions has been chosen:

$$G_{vs}(s) = \frac{K_{vs}}{\tau_a s + 1} \qquad (2)$$

$$G_{cs}(s) = K_{cs} = K_{vs} R_a, \qquad (3)$$

where τ_a is the electromagnetic time-constant of the respective armature circuit section.

After substitution of Eqs. (2) and (3) in Eq. (1), for the feedback signal V_{ef} the following expression is obtained:

$$V_{ef}(s) = \frac{K_{vs}}{\tau_a s + 1} \big[E(s) + I_1(s) R_a (\tau_a s + 1) \big] -$$

$$- K_{vs} R_a I_1(s). \qquad (4)$$

From Eq. (4) the transfer function of the back EMF voltage sensor receives the following form:

$$G_{es}(s) = \frac{V_{ef}(s)}{E(s)} = \frac{K_{ef}}{\tau_{ef} s + 1}, \qquad (5)$$

where the gain and the time-constant of the back EMF voltage feedback are defined respectively as:

$$K_{ef} = K_{vs} \qquad (6)$$

and

$$\tau_{ef} = \tau_a. \qquad (7)$$

Inserting a filter with a time-constant τ_{ef} into the feedback loop enhances the drive system noise protection.

In electric drive systems with single-zone speed regulation, the represented back EMF voltage sensor can be used for sensorless control, replacing the respective electromechanical speed sensor, fixed on the motor shaft.
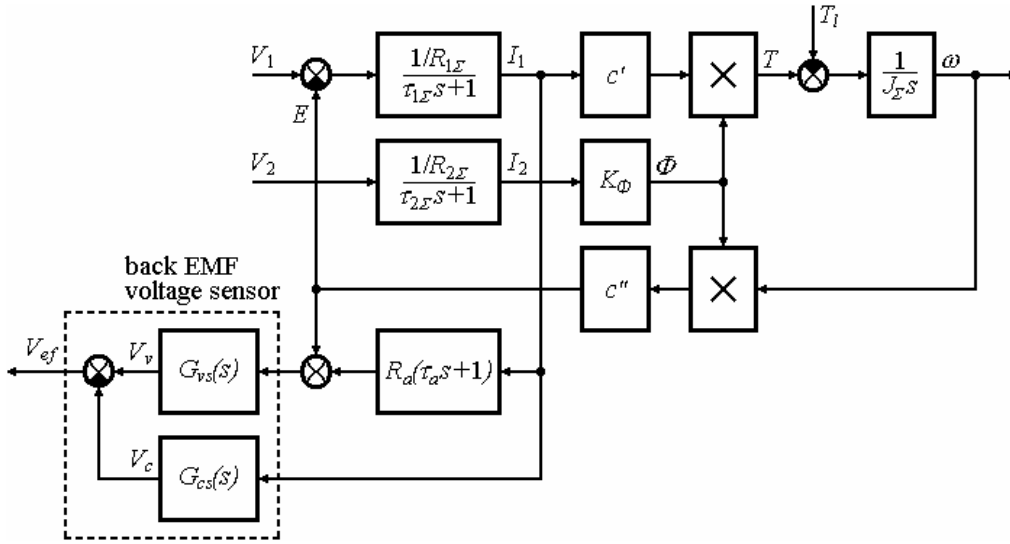
Fig. 2. Block diagram illustratig the prosses of obtaining information about the back EMF voltage

IV. CONTROL LOOPS OPTIMIZATION

The subsistems are of dual-loop type, with subordinated regulation. Control loops opitimization is carried out following the resepctive critera, providing for the necessary performnce [1], [3]. Controllers tuning is done sequentially, starting from the innermost loops.

The armature current loop optimization can be carried out taking into account or neglecting the internal feedback by the back EMF voltage. In the general case this depends on the ratio between the two big time-constants $\tau_{m\Sigma}$ and $\tau_{1\Sigma}$. The bigger summary electromechanical time-constant $\tau_{m\Sigma}$, the lower is the error from neglecting the back EMF voltage influence.

In the case of neglecting the internal feedback by the back EMF voltage, the transfer function of the armature current controller assumes the following form:

$$G_{c_1c}(s) = \frac{R_{1\Sigma}(\tau_{1\Sigma}s+1)}{2K_{p_1}K_{c_1f}\tau_{\mu c_1}s}, \qquad (8)$$

where $\tau_{\mu c_1} = \tau_{p_1} + \tau_{c_1f}$ is the summary small time-constant of the loop, not subject to compensation.

Reading the back EMF voltage influence, the current controller transfer function is as follows:

$$G_{c_1c}(s) = \frac{\tau_{1\Sigma}\tau_{m\Sigma}s^2 + \tau_{m\Sigma}s + 1}{2K_{p_1}K_{c_1f}\tau_{\mu c_1}\tau_{m\Sigma}s^2/R_{1\Sigma}}. \qquad (9)$$

One of the used versions for the first subsystem external loop optimization leads to the following transfer function of the speed controller:

$$G_{sc}(s) = \frac{4\tau_{m\Sigma}\tau_{\mu s}s^2 + \tau_{m\Sigma}s}{8K_m K_{sf}R_{1\Sigma}\tau_{\mu s}^2 s^2/K_{c_1f}}, \qquad (10)$$

where: $\tau_{\mu s} = 2\tau_{\mu c_1}$; $K_m = 1/c'\Phi_{\text{nom}}$.

For the transfer function of the excitation currnent controller the following equation is obtained:

$$G_{c_2c}(s) = \frac{R_{2\Sigma}(\tau_{2\Sigma}s+1)}{2K_{p_2}K_{c_2f}\tau_{\mu c_2}s}, \qquad (11)$$

where $\tau_{\mu c_2} = \tau_{p_2} + \tau_{c_2f}$ is the summary small time-constant of the respective loop, not subject to compensation.

After optimization of the back EMF voltage loop, an integral controller is achieved, with the following transfer function:

$$G_{ec}(s) = \frac{K_{ec}}{\left[2\tau_{\mu c_2} + \tau_a + \sqrt{\left(2\tau_{\mu c_2}+\tau_a\right)^2 + \tau_a^2}\,\right]s}, \qquad (12)$$

where $K_{ec} = K_{c_2f}/K_{ef}K_{\Phi}c''\omega$.

Using the MATLAB/SIMULINK software package a number of computer simulation models have been developed of systems with dual-zone speed regulation for various tunings of the control loops.

Detailed investigations have been carried out in the respective dynamic and static regimes at diverse loading, disturbances and work conditions.

V. SOME SIMULATION RESULTS

Fig. 3 shows some of the time-diagrams, obtained through inverstigations of the system in the first zone of speed regulation. The transient start process is shown, as well as operaton at steady state regime with rated load torque applied
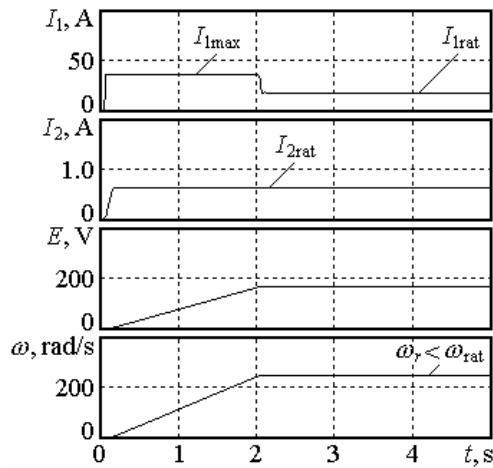
Fig. 3. Time-diagrams about the first zone of speed regulation

to the motor shaft. The set motor speed is $\omega_r < \omega_{rat}$ and the starting armature current is limited to the maximum admissible value of $I_{1\max}$, which provides a maximum starting
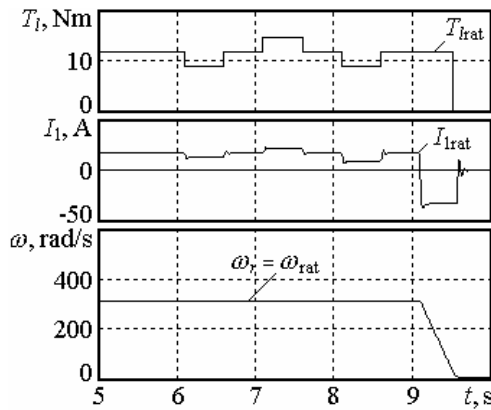
Fig. 4. Speed stabilization and braking regime

motor torque. The excitation current is of a consntant value of $I_2 = I_{2rat}$.

Fig. 4 represents speed stabilization in the presence of dis-
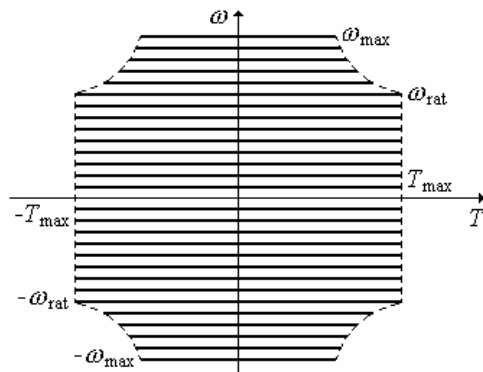
Fig. 5. Torque/speed curves of the four-quadrant drive system

turbances. The load torque is equal to the rated value T_{lrat}, while the disturbances applied sequentially are $\Delta T_l = -25\%$, $\Delta T_l = +25\%$ and $\Delta T_l = -25\%$, respectively. The braking regime is illustrated for initial motor speed of $\omega_r = \omega_{rat}$.

Fig. 5 shows torque/speed curves of the four-quadrant electric drive system, where $\omega_{\max}$ is the upper bound of the speed regulation range and $T_{\max}$ is the maximum motor torque. At $\omega_r > \omega_{rat}$ excitation cuttent in steady state regime is $I_2 < I_{2rat}$, while the admissible armature current is auto-
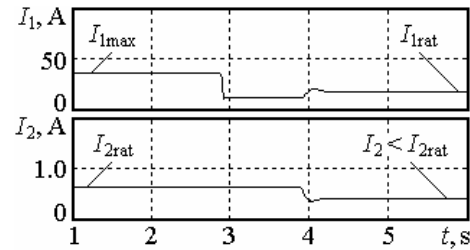
Fig. 6. Change of the motor currents in the zone with flux weakening

matically limited below the $I_{1\max}$ value.

The change of the motor currents in the zone of speed regulation with flux weakening control is represented in Fig. 6.

VI. CONCLUSION

Computer simulation models of electric drive systems with dual-zone speed regulation have been developed, allowing investigations at various loads and disturbances applied to the motor shaft.

Optimization of the control loops by different criteria has been carried out, as well as analysis of the dynamic and static regimes for the respective versions of controllers tuning.

The rated parameters of the separately excited DC motor are as follows: $P_{rat} = 3.4\,\text{kW}$, $V_{1rat} = 220\,\text{V}$, $I_{1rat} = 17.6\,\text{A}$, $\omega_{rat} = 314\,\text{rad/s}$.

The simulation models and the results obtained from the respective investigations can be used as in optimization and tuning of drive systems of the class discussed above, so as illustration in the process of teaching about such types of electric drives.

REFERENCES

[1] A. V. Basharin, V. A. Novikov, G. G. Sokolovskiy, *Control of electric drives*, Sankt Petergburg, Energoizdat, 1982 (in Russian).
[2] U. Keuchel, R. M. Stephan, *Microcomputer-based adaptive control applied to thyristor-driven dc motors*, London, Springer-Verlag, 1994.
[3] N. Mohan, *Electric drives – an integrative* approach, Minneapolis, MNPERE, 2003.
[4] C. Ong, *Dynamic simulation of electric machinery*, New Jersey, Prentice Hall, 1998.
[5] M. R. Mikhov, "Control of dual-motor drive systems", *ICMIT 2001 Conference Proceedings*, pp. 198-203, Yamaguchi, Japan, 2001.